Building Technologies & Urban Systems Division
Energy Technologies Area
Lawrence Berkeley National Laboratory

A simulation-based method to analyze fan coil unit fault impacts

Yimin Chen, Zhelun Chen, Guanjing Lin, Jin Wen, Jessica Granderson

Energy Technologies Area
June, 2022

Acknowledgements:

The authors would like to thank Christopher Weyandt and Raphael Vitti of the Sustainable Berkeley Lab for their significant contributions to this case study. This work was supported by the Assistant Secretary for Energy Efficiency and Renewable Energy, Building Technologies Office, of the U.S. Department of Energy, under Contract No. DE-AC02-05CH11231.

A simulation-based method to analyze fan coil unit fault impacts

Yimin Chen, PhD
Associate Member ASHRAE

Zhelun Chen, PhD
Associate Member ASHRAE

Guanjing Lin, PhD
Member ASHRAE

Jin Wen, PhD
Member ASHRAE

Jessica Granderson, PhD

ABSTRACT

Fan coil units (FCUs) are decentralized air-conditioning devices to locally condition zone air. In the U.S. and Europe, FCUs are widely deployed in diverse types of buildings such as offices, hotels, schools, and residential apartments because of their low cost and easy installation. The abnormal operation of FCUs due to faults or malfunctioning components may cause significant energy waste and degrading thermal comforts. However, faults occurring in FCUs have been seldom investigated. A systematic analysis of fault impacts of FCUs would enable a better understanding of fault impacts, an efficient development of fault diagnostics approaches, and an improvement of FCUs monitoring system design. In this paper, we used a FCU simulation model, which was developed in the HVACSIM+ environment from a previous study to evaluate FCU fault impacts. Five common faults with different intensities were simulated within a one-year time window to generate fault inclusive operation data. We employed a bottom-up fault impact analysis framework. Fault effects on multiple measurements were firstly evaluated to obtain fault symptom occurrence probability distributions which quantify measurements' sensitivities. Secondly, fault thermal comfort impact and fan power energy consumption impact were assessed. Lastly, the result from fault thermal comfort impacts and energy penalties was used to rank FCU faults.

INTRODUCTION

Heating, ventilation and air conditioning (HVAC) systems provide satisfied thermal comforts and indoor air quality to occupants, and represent a large portion of the energy consumption in buildings. The reliable operation and efficient monitoring of HVAC systems have drawn significant attention because hardware and software faults in equipment may cause system operating abnormalities, energy consumption wastes, thermal comfort degradation and system lifespan reduction. For example, it is estimated that faults in HVAC systems cause 40% more primary energy consumption in commercial buildings in the United States (*Annual Energy Outlook 2020 with projections to 2050*, 2020).

With regard to HVAC fault research activities, the evaluations of HVAC system fault impacts on multiple factors have become one of active areas (Li and O'Neill, 2019). The analysis of fault impacts often includes impacts on multiple metrics such as energy consumption, financial costs, thermal comforts, system operation performance and so on. Meanwhile, a large body of literature has investigated fault impacts on various HVAC equipment. For instance, Comstock et al. investigated eight common faults in a centrifugal chiller in a laboratory environment (Comstock et al., 2001). A total of 13 measurements were used to evaluate the measurement sensitivity under chiller's faulty operation.

Yimin Chen is a Senior Scientific and Engineering Associate in the Building Technology & Urban Systems Division at Lawrence Berkeley National Laboratory, Berkeley, CA. **Zhelun Chen** is a Research Scientist in the Department of Civil, Architectural and Environmental Engineering at Drexel University, Philadelphia, PA. **Guanjing Lin** a Principal Scientific and Engineering Associate in the Building Technology & Urban Systems Division at Lawrence Berkeley National Laboratory Berkeley, CA. **Jin Wen** is a Professor in the Department of Civil, Architectural and Environmental Engineering at Drexel University, Philadelphia, PA. **Jessica Granderson** a Staff Scientist in the BuildingTechnology & Urban Systems Division at Lawrence Berkeley National, Berkeley, CA.

Breuker et al. identified important faults and their performance impacts on rooftop units (RTUs) (Breuker and Braun, 1998).

However, compared with other HVAC systems such as chiller plants, AHUs or VAV terminal units, efficient monitoring of fan coil units' (FCUs) operation is insufficient due to a diverse deployment. FCUs are simple and decentralized air-conditioning devices which are primarily used to locally condition the air in zones. Compared with other HVAC systems, FCUs can be easily and flexibly deployed in buildings where the space is limited to install ducts (Thornton and Wagner, 2012). As a result, FCUs are widely used in various types of buildings including offices, hotels, schools, as well as residential apartments in the U.S and in Europe. To the authors' best knowledge, the evaluation of FCUs' fault impacts is inadequate due to difficulty of performing comprehensive field investigations.

In this study, we employed a bottom-up fault impact analysis framework to evaluate FCU fault impacts on the critical measurements, energy consumption as well as zone thermal comfort. Instead of performing field investigations and laboratory tests, we simulated faults based on a FCU simulation platform which was previously developed by the HVACSIM+ software tool (Pourarian et al., 2017). Faults at different intensities were imposed to obtain fault inclusive operation data within a whole year time scope to fully evaluate fault symptom occurrence probability distributions on key measurements. Additionally, annual energy consumption penalty and zone thermal comfort impacts are quantified as well. A fault ranking is presented based on the fault impacts on energy consumption and thermal comfort.

METHODOLOGY

In the proposed bottom-up fault impact analysis framework, an evaluation of local fault impacts (i.e., fault effects on individual measurements) was first performed. Then, the evaluation of global fault impacts (i.e., fault impact on the overall operating performance such as zone thermal comforts and energy consumption) was carried out. As shown in Figure 1, the evaluation framework of FCU fault impacts follows the following five major steps as 1) simulation platform setup, fault free data generation and the ground truth establishment, 2) faults imposition and fault data collection, 3) fault effect analysis on individual measurements, 4) fault thermal comfort impact analysis and 5) fault energy impact analysis. The detailed description of each step will be illustrated below.

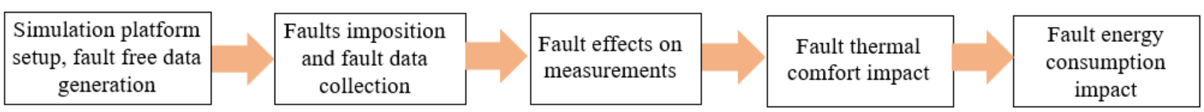

Figure 1 Fault impact analysis workflow

Simulation setup and fault free data collection

First, we set up the simulation platform by determining the control sequence and setting the simulation parameters. In this study, a previously developed vertical four pipe hydronic FCU model based on the HVACSIM+ software tool (Clark and May, 1985), was used to impose faults. Compared with other fault impact studies which used EnergyPlus, the FCU fault model developed by the HVACSIM+ software tool includes more detailed dynamic models such as damper and valve dynamics, and allows the HVAC and control systems to be simulated with a much finer time step (as low as 2.5 second), so that the dynamic operating performance of the equipment can be captured more accurately. Certain fault symptoms, such as how a stuck damper (say, stuck at 0% open) would drive the control signal to be at a saturated value (i.e., 100% open), could only be accurately reflected if such dynamics are modeled with a time step that is less than a minute. Controllers in the field often send control signals with a time step of five seconds or so.

The developed FCU simulation platform enables the imposition of various faults in the actuators, sensors, static parts and control sequence. Multiple measurements such as temperature, humidity and air flow rate, as well as control signals can be monitored. The equipment physical configuration is illustrated in the graphic in Figure 2. In the figure, the red color points represent the key measurements that were used in this study.

The control sequences were set for the occupied period (i.e., 6:00AM to 6:00PM each weekday). Four separate control sequences for fan control, outdoor air damper control, cooling coil valve control as well as heating coil valve control were developed, based on common ones observed in the field, as described below.

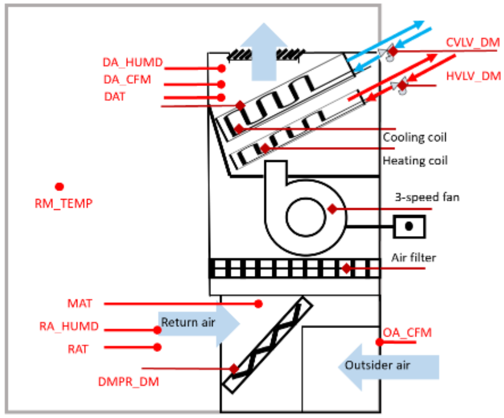

Figure 2 FCU configuration schematic

In the FCU model, a 3-speed fan with "Automatic On/Off" (Auto) mode was modeled. The operation of fan on/off status and fan speed is controlled according to the cooling PID loop and heating PID loop. The outdoor air damper was controlled to maintain a minimum damper position at 30% open position during the operation. The zone cooling setpoint was set to 22.5 °C (73 °F). Two PID control loops were used to adjust the cooling coil valve position and the heating coil valve position respectively. During operation, if the zone temperature was higher than the cooling setpoint, the FCU switched to the "cooling" mode. When the zone temperature fell 0.56°C (2 °F) below the cooling setpoint, the cooling PID loop was disabled and the valve fully closed. The zone heating setpoint was set to 19.7 °C (67 °F). If the zone temperature was lower than the heating setpoint, the FCU switched to the "heating" mode. When the zone temperature was 0.56°C higher than the heating setpoint, the heating PID loop was disabled and the valve fully closed.

The TMY weather data file for Des Moines, IA U.S. was used as the weather inputs. This weather data was used because the FCU model was developed and validated by using the testing platform in the Iowa Energy Center.

The fault free simulation was performed to obtain one year fault free data. After the fault free data was collected, we validated the fault free data by using the established validation protocol (Casillas et al., 2020) to obtain the ground truth.

Fault imposition and faulty data collection

In this preliminary study, we imposed five faults (i.e., cooling coil leakage fault, heating coil stuck fault, control unstable fault, and filter restriction fault) with various intensity levels in the developed FCU model. Consequently, a total of 17 fault test cases were performed. In order to fully evaluate maximum fault impacts on energy consumption and zone thermal comfort, we imposed continuous faults on the FCU model, i.e., a fault occurs on the FCU during the entire schedule period in one day within one year scope. The fault description, fault intensity level, as well as imposition methods are described in Table 1.

Fault symptom analysis on measurements

In an HVAC system, various sensors and control signals can be employed to monitor the system's dynamic operation performance. In the early stage of HVAC system fault diagnostics, the observable fault symptoms on various measurements were widely used by operators to judge a system's operation, as well as determine system operational abnormalities. This heuristic process generated qualitative measures such as some linguistic expressions like 'small', 'normal' and 'large' for empirical fault diagnostics (Isermann, 2005), and further evolved to some fault diagnostics approaches such as rule-based fault diagnostics (Schein and Bushby, 2006) and the expert system (Kaldorf and Gruber, 2002). Thanks to the rapid development of sensor techniques and achievements of data-driven techniques, an increasing volume of sensors has been deployed in the HVAC system, and more data can be easily collected for developing advanced data-driven fault diagnostics solutions. However, one question -- the sensitivity of a measurement under a fault -- remains to be addressed to evaluate fault impacts, assess the fault detectability, effectively develop fault diagnostics inference approaches, as well as optimally deploy sensors.

Table 1. List of Fault Tests

Component Type	Fault Name	Fault Intensity	Method of Fault Imposition (Number of cases)
Heating valve	Stuck	Stuck at 0%, 20%, 50%, 80%, 100%	Assign a fixed simulated controlled device position (5)
Cooling Valve	Leaking	20%, 50%, 80% of the max flow (0.36kg/s)	Assign a water flow rate when fully closed (3)
Control	Control unstable	Not applied	Decrease all proportional bands to their 10% respectively (1)
Filter	Restriction	Outlet resistance +23.45%, +56.25%, +400% (corresponding to 10%, 20%, 50% flow rate reduction at the same pressure difference)	Increase air flow pressure resistance (3)
Outdoor air damper	Stuck	Stuck at 0%, 20%, 50%, 80%, 100%	Assign a fixed simulated controlled device position (5)

In order to quantify the measurement sensitivity under each fault, we propose to evaluate the symptom occurrence likelihood, i.e., the fault symptom occurrence probability distribution under each fault type. For a HVAC system, the observation likelihood of fault symptoms on each measurement can be affected by various factors such as weather conditions, fault intensity, equipment control sequence, as well as occupants' interactivity. In this study, we evaluated the fault symptom occurrence probability for each measurement under different weather conditions (i.e., outdoor air temperature, OAT), and fault intensities. The OAT was used because it plays a critical role to affect the zone load, and is used in the part of control sequence. To achieve this goal, four steps were carried out as illustrated below.

First, the normal value of the measurement y is calculated from normalizing fault free data under different OAT conditions. The OAT is equally binned and the data during fault free operation is normalized by using z-score method which has been mostly employed by data-driven methods as. The number of bins affects the generation of baseline data. In this study, the number of OAT bins was set to ten after taking two considerations as 1) the FCU operation status within one binned window should be stable; and 2) the sample size within one binned window should be large enough to reach a statistical significance.

$$Z = \frac{y-\mu}{\sigma}$$

where μ is the mean value of measurement, and σ is the standard deviation of the measurement within the binned OAT window respectively.

Secondly, after normalizing the fault free data, mean value and standard deviation of each measurement under each binned OAT window can be obtained. Consequently, the symptom can be determined by comparing if the absolute difference between the observed value and the mean value of the measurement is higher than the standard deviation of the measurement as given in Eq. 1.

$$\left|y_o(i) - \bar{y}\right| > t\times\sigma \qquad (1)$$

where, y_o is the observed time series data, $\bar{y}$ is the mean value of the baseline data (i.e., the normal value of the measurement), σ is the standard deviation of the baseline data, t is the threshold value (1, 2, …). In this study, t equaled one as the determination of an observable fault symptom. That is to say, when the operation data is higher or lower than one standard deviation, this data is labelled as a symptom of the measurement.

Further, in this step, a symptom's direction can be determined to be positive or negative to represent the direction of a measured data, i.e., a difference (ε) is higher than one standard deviation or lower than one negative standard deviation.

Thirdly, when a fault symptom is recorded within the binned OAT window, the fault occurrence frequency can be obtained by Eq. 2.

$$P\left(OP_{OAT}\right) = \frac{\sum num\_fault\_sym}{\sum OP\_time} \qquad (2)$$

where num_fault_sym is the number of the observed fault symptom samples, and OP_time is the total data recorded during the operation time period within the binned OAT window.

Lastly, the total probability distribution of fault symptom occurrence is calculated. There are multiple probability weighting approaches that can be used to calculate the total probability (Cleman and Winkler, 1999). In this study, we employ the Bayesian approach (Olshausen, 2004) to calculate the total probability distribution of a symptom for each fault type with various fault intensity levels as given in Eq. 3.

$$P\left(OP_{OAT}\right) = \sum_{i}^{num\_bin\_window} P\left(OP_{OAT}\right)_i P\left(OP_{OAT}\right)_i \qquad (3)$$

where $P\left(OP_{OAT}\right)_i$ is the symptom occurrence probability the under i^{th} binned OAT window as given in Eq. 3, $P\left(OP_{OAT}\right)_i$ is the operating ratio of the i^{th} binned OAT under all operating time, num_bin_window is the total number of binned windows.

Fault zone thermal comfort impact analysis

The zone temperature setpoint unmet ratio can be used to evaluate the zone thermal comfort (Lu et al., 2021). In this study, we evaluated the percentage of time period when zone temperature setpoints are not met under each fault as given in Eq. 4. This means that the zone temperature can be either higher than the cooling setpoint or lower than the heating setpoint.

$$Pct_{annual\_spt\_unmet} = \frac{\sum_{t=1}^{spt\_unmet\_opt\_min} t}{\sum_{t=1}^{opt\_min} t} \times 100\% \qquad (4)$$

where $spt\_unmet\_opt\_min$ is the annual number of operation minutes when the zone temperature setpoint was not met, and opt_min is the annual total operation minutes.

Fault energy consumption impact analysis

In this study, fault energy consumption impact was evaluated by calculating the percentage change of the daily fan electricity consumption and annual electricity consumption caused by various faults respectively, as given in Eq. 5.

$$Pct_{fan\_power} = \frac{\sum_{t=1}^{opt\_hour} P\_fault \times t - \sum_{t=1}^{opt\_hour} P\_fault\_free \times t}{\sum_{t=1}^{opt\_hour} P\_fault\_free \times t} \times 100\% \quad (5)$$

where, P_fault is fan power consumption under faulty operation, P_fault_free is fan power consumption under fault-free operation, and opt_hour is the total operation hours.

RESULTS AND DISCUSSION

In the study, a total of ten measurement data (including seven types of sensor data and three types of control signals), which are commonly collected in the monitoring system, was used to assess fault effects on each measurement. The measurements are listed in Table 2.

Table 2. List of Measurements

No.	Data Point Name	Description	No.	Data Point Name	Description
1	MAT	Mixed air temperature	6	CVLV_DM	Cooling coil valve control signal
2	DAT	Discharge air temperature	7	HVLV_DM	Heating coil valve control signal
3	RAT	Return air temperature	8	DMPR_DM	Outdoor air damper control signal
4	DA_CFM	Discharge air flow rate	9	DA_HUMD	Discharge air humidity
5	OA_CFM	Outdoor air flow rate	10	RA_HUMD	Return air humidity

The simulation time step was set to 5 seconds, which is a common time interval used by field controllers to update their output, and the simulation output rate was set to 1 minute interval, which is the lowest measurement intervals that can be used in the field. Consequently, for fault free test case and each fault test case, the simulation generates 187,920 operating minutes within 261 operating days in one year. The OAT data from the operating time is binned into ten windows with 6 °C (10.8 °F) binned size. Table 3 provides the median binned OAT values, operation duration and operation duration ratio within each binned window.

In this paper, we employ the heating coil valve stuck fault (FCU_VLVStuck_Heating) as an example to demonstrate the total symptom probability results for each measurement. This fault was simulated under five intensity levels as 0%, 20%, 50%, 80%, and 100% respectively.

Table 3. Operation Data for Evaluating Fault Symptoms

Bin No.	Bin #1	Bin #2	Bin #3	Bin #4	Bin #5	Bin #6	Bin #7	Bin #8	Bin #9	Bin #10
Median OAT [°C(°F)]	-20.3 (-4.5)	-14.4 (6.1)	-8.5 (16.7)	-2.5 (27.5)	3.4 (38.1)	9.4 (48.9)	15.7 (60.3)	21.3 (70.4)	27.2 (81.0)	33.1 (91.6)
Operation duration (minutes)	2445	7580	11919	17665	31987	21548	21127	32737	32640	8272
Operation duration ratio (%)	1.3	4.0	6.3	9.4	17.0	11.5	11.2	17.4	17.4	4.4

First, the symptom occurrence probability under each binned OAT window was calculated by using Eq. 2. For various fault intensities, the occurrence probability distribution range for each measurement are given in Table 4 and 5. For this fault, the symptom observability is highly dependent on the weather condition. The symptom occurrence probability may increase when the OAT increases. For example, under Bin #7 to #10 windows (i.e., the OAT ranges from 12.7 °C (54.9 °F) to 36.1 °C (97.0 °F)), the maximum occurrence probabilities of positive symptoms for eight measurements can reach 97% to 100% respectively.

Table 4. Positive Symptom Occurrence Probability under Each Binned OAT Window (%)

Data Point Name	Bin #1	Bin #2	Bin #3	Bin #4	Bin #5	Bin #6	Bin #7	Bin #8	Bin #9	Bin #10
MAT	0	0-18	0-12	0-14	0-23	0-50	4-98	5-99	12-100	11-100
DAT	0-100	0-78	0-73	0-100	0-100	9-100	19-100	18-100	14-100	16-100
RAT	0-9	0-44	0-46	2-59	1-74	4-94	6-99	3-100	4-100	16-100
CVLV_DM	0	0-26	0-34	1-51	1-72	2-92	1-99	16-99	16-99	9-100
HVLV_DM	0-86	0-92	0-97	0-90	0-87	0-35	0-7	0	0	0
DA_CFM	0-86	10-92	27-96	43-88	59-84	4-91	0-97	0-99	0-99	4-100
OA_CFM	0-86	10-92	27-96	43-88	59-84	4-91	0-97	0-99	0-99	4-100
DMPR_DM	0	0	0	0	0	0	0	0	0	0
DA_HUMD	0-100	0-100	0-98	0-97	0-92	0-31	0-13	0-15	0-16	0-16
RA_HUMD	30-100	46-100	44-93	8-45	10-43	1-19	0-20	0-15	0-12	0-14

Table 5. Negative Symptom Occurrence Probability under Each Binned OAT Window (%)

Data Point Name	Bin #1	Bin #2	Bin #3	Bin #4	Bin #5	Bin #6	Bin #7	Bin #8	Bin #9	Bin #10
MAT	62-100	59-100	56-99	46-94	26-86	6-44	0-13	0-10	0-15	0-6
DAT	0-100	0-100	0-98	0-97	0-93	0-33	0-13	0-14	0-14	0-16
RAT	1-100	1-100	0-100	0-96	3-89	2-39	0-12	0-2	0-6	0-34
CVLV_DM	0	0	0	0	0	6-58	0-25	0-12	0-9	0-11

HVLV_DM	10-100	5-98	0-99	8-99	0	0	0	0	0	0
DA_CFM	0-87	0-78	0-55	4-47	8-30	6-16	0-5	0	0	0
OA_CFM	10-94	5-88	0-55	4-47	8-30	6-16	0-5	0	0	0
DMPR_DM	0-87	0-79	0-25	0-4	0-2	0	0	0	0	0
DA_HUMD	0-99	0-78	0-73	0-100	0-100	6-100	19-100	18-100	14-100	17-100
RA_HUMD	0	0-20	0-27	3-36	8-42	11-57	15-50	19-98	14-100	9-100

Then, the total symptom occurrence probability for each measurement under a specific fault intensity level can be calculated by using Eq. 3. Figure 3 shows total probability values for positive/negative symptoms on the ten measurements for the FCU_VLVStuck_Heating fault under five intensities respectively.

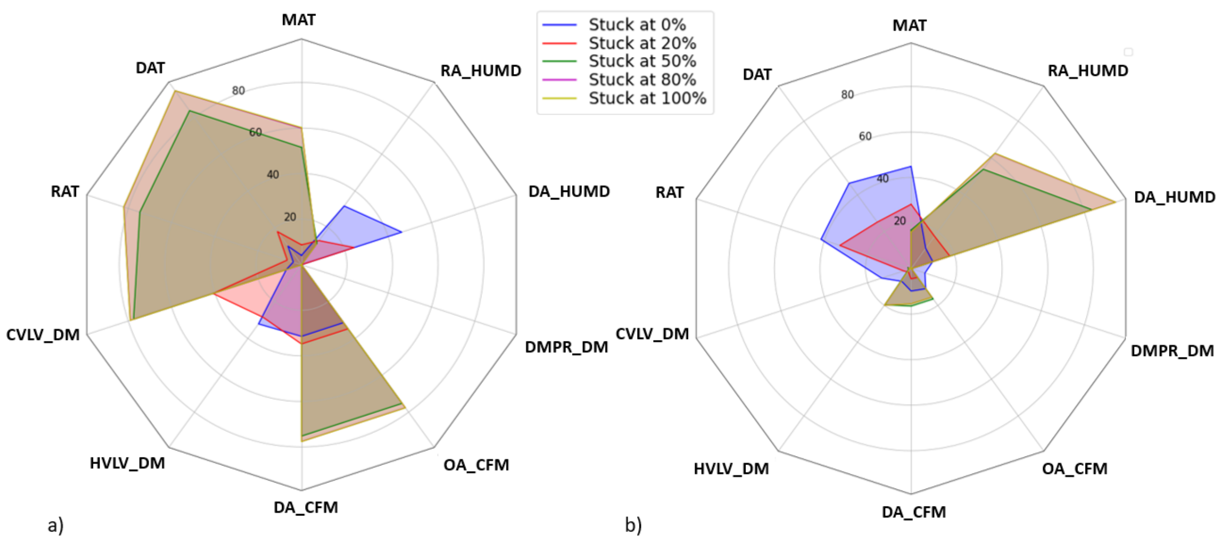

Figure 3 a) Positive symptom occurrence probability, and b) Negative symptom occurrence probability

It can be seen that the observability of fault symptom is very sensitive to the fault intensities because the total symptom occurrence probability distributions range widely according to various fault intensities. Eight measurements (i.e., CVLV_DM, RAT, DAT, MAT, OA_CFM, DA_CFM, DA_HUMD and RA_HUMD) have significantly high total occurrence probability values (i.e., the minimum total occurrence probability is higher than 50%) under high intensity levels. For example, for the DAT measurement, the positive symptom total occurrence probability range is from 83% to 94% when the valve is stuck higher than a 50% position. While for this measurement, the negative symptom total occurrence probability range is from 25% to 46%. The symptom occurrence probability for two measurements, such as HVLV_DM and DMPR_DM, are relatively lower. This is due to fault symptoms on some measurements that can be hardly observed because the measurements are relatively isolated from the fault causes, or because fault effects on some measurements can be minimized by specific control sequences in some actuators. For example, for the DMPR_DM measurement (i.e., damper control signal), the negative symptom total occurrence probability is 6% when the heating valve is stuck at a 0% position, and occurrence probability is near or equal 0% for other intensity levels.

This is because the FCU damper control cannot compensate for the abnormal operation caused by the fault. Another example is for the HVLV_DM measurement (i.e., the valve control signal). When the heating coil valve is stuck at a higher position, The occurrence probability values are 0% for the negative symptom on the HVLV_DM measurement. This means that the valve is not controlled to decrease the valve position. This is because the cooling coil valve position is increased to maintain the zone temperature, and consequently lead to a simultaneous heating and cooling operational status.

Figure 4 shows the thermal comfort impact results. It can be seen that the FCU_VLVStuck_Heating fault may cause significant zone thermal comfort impacts. For example, when the FCU_VLVStuck_Heating fault is at 100% intensity level, the annual zone temperature setpoint unmet time reaches 63% of total operation time. The FCU outdoor air damper stuck (FCU_OADMPRStuck) fault may also cause significant zone thermal comfort impact when the fault intensity is high. For example, when the outdoor air damper is stuck at 100%, the annual zone temperature setpoint unmet time reaches 43% of total operation time. Contrarily, the FCU filter restriction fault (FCU_FilterRestriction) may cause minor zone thermal comfort impact as the maximum annual zone temperature setpoint unmet time is only 3% of total operation time when the filter is 50% blocked.

Figure 4 shows the fault energy impact results. It can be seen that the FCU_VLVStuck_Heating fault at 100% intensity level causes the most serious energy impact. This fault leads the FCU to be operated at a simultaneous heating and cooling status. The supply air fan speed is increased to provide more cooling so that the excessive cooling load caused by this fault can be compensated for. Under this fault, the annual fan power energy consumption increases by 433% compared to the baseline data.

On the other hand, for the FCU cooling coil valve leaking (FCU_VLVLeak_Cooling) fault causes negative impact on fan power energy consumption, i.e., the annual fan power energy consumption decreases by 13% compared to the baseline. This is because under the FCU_VLVLeak_Cooling fault, the supply air fan does not operate at a higher speed to provide more cooling to the zone. However, during the heating season, this may cause extra heating energy consumption.

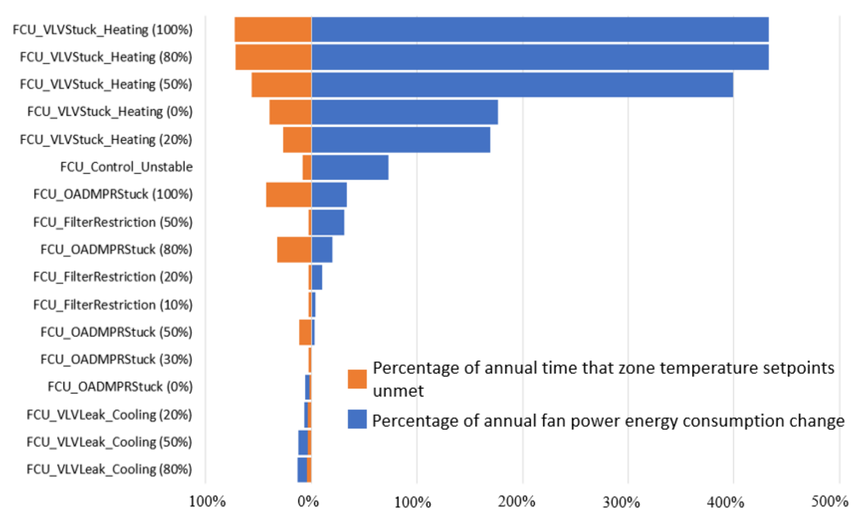

Figure 4 Fault zone thermal comfort impact and energy consumption impact

From Figure 4, it can be seen that the FCU_VLVStuck_Heating fault may cause severe impacts on both energy consumption and zone thermal comfort. With respect to fan energy consumption, the second severe fault is the FCU control unstable (FCU_Control_Unstable) fault. The FCU outdoor air damper stuck fault may only have significant impact on the zone thermal impact when the intensity level is high (e.g., stuck at 80% and 100% position respectively). The filter restriction fault and the cooling coil valve leak fault have relatively lower impacts on both the zone thermal comfort and fan energy consumption.

CONCLUSION AND FUTURE WORK

In this study, we used a previously developed FCU simulation platform to evaluate fault impacts on FCUs. Five common hardware and software faults were imposed to obtain one year fault-inclusive system operation data. We employed the bottom-to-up method to systematically evaluate FCU fault impacts.

First, the fault effects on the critical measurements were quantified by using fault symptom occurrence probability distributions. The results show that fault symptom occurrence probability could be affected by system operational conditions such as weather conditions, as well as fault intensity levels. This result would enable the effective deployment of sensors to enhance monitoring efficiency. Moreover, the obtained fault symptom occurrence probabilities can facilitate the development of certain probability-based fault diagnosis methods, such as Bayesian Network based fault diagnosis. Secondly, in terms of fault impacts on zone thermal comforts, our study shows the faults simulated in this study do not cause significant occurrences when the zone temperature setpoint is unmet, from an annual perspective. Among all the faults simulated, the FCU_VLVStuck_Heating fault and FCU_OADMPRStuck fault can cause relatively large thermal comfort impacts. Lastly, with respect to the energy consumption penalty, our study shows that fan power consumption changes may range widely depending on the various types of fault and fault intensity levels. The FCU_VLVStuck_Heating fault at various intensities can cause significant increases on fan power consumption.

Our future work includes a further investigation on control operating performance in the FCU so that a comprehensive symptom occurrence probability distribution on various measurements can be obtained. Besides, we may include cooling and heating consumption analysis and other metrics in later works.

ACKNOWLEDGMENTS

This work was supported by the Assistant Secretary for Energy Efficiency and Renewable Energy, Building Technologies Office, of the U.S. Department of Energy under Contract No. DE-AC02-05CH11231.

REFERENCES

U.S. Energy Information Administration. *Annual Energy Outlook 2020 with projections to 2050 (No. AEO2020)*, 2020. Washington, DC.

Breuker, M.S., Braun, J.E., 1998. Common faults and their impacts for rooftop air conditioners. *HVAC&R Research*. 4, 303–318.

Casillas, A., Lin, G., Granderson, J., 2021. Curation of Ground-Truth Validated Benchmarking Datasets for Fault Detection & Diagnostics Tools. from https://escholarship.org/uc/item/9cz491j6 (accessed 11.20.21).

Clark, D.R., May, W.B., 1985. HVACSIM+ building systems and equipment simulation program - user's guide (NBSIR-85/3243). National Bureau of Standards, Building Equipment Division, Washington, DC.

Cleman, R.T., Winkler, R.L., 1999. Combining Probability Distributions From Experts in Risk Analysis. *Risk Analysis*. 19, 187–203.

Comstock, M.C., Braun, J.E., Groll, E.A., 2001. The sensitivity of chiller performance to common faults. *HVAC&R Research*. 7, 263–279.

Isermann, R., 2005. *Fault-Diagnosis Systems: An Introduction from Fault Detection to Fault Tolerance*. Springer Science & Business Media, Germany.

Kaldorf, S., Gruber, P., 2002. Practical experiences from developing and implementing an expert system diagnostic tool /Discussion. *ASHRAE Transactions*. 108, 826.

Li, Y., O'Neill, Z., 2019. An innovative fault impact analysis framework for enhancing building operations. *Energy and Buildings*. 199, 311–331.

Lu, X., Fu, Y., O'Neill, Z., Wen, J., 2021. A holistic fault impact analysis of the high-performance sequences of operation for HVAC systems: Modelica-based case study in a medium-office building. *Energy and Buildings*. 252, 111448.

Olshausen, B.A., 2004. *Bayesian probability theory*. The Redwood Center for Theoretical Neuroscience, Helen Wills Neuroscience Institute at the University of California at Berkeley, Berkeley CA.

Pourarian, S., Wen, J., Veronica, D., Pertzborn, A., Zhou, X., Liu, R., 2017. A tool for evaluating fault detection and diagnostic methods for fan coil units. *Energy and Buildings*. 136, 151–160.
Schein, J., Bushby, S.T., 2006. A hierarchical rule-based fault detection and diagnostic method for HVAC systems. *HVAC&R Research*. 12, 111–125.
Thornton, B., Wagner, A., 2012. *Variable Refrigerant Flow Systems*. U.S. General Services Administration, San Francisco, CA.